Numerical computation of the damping and stiffness coefficients of the classical and magnetorheological squeeze film damper

Petr Ferfecki[1,2,*], *Jaroslav* Zapoměl[2,3], *Michal* Šofer[2], *František* Pochylý[4], *Simona* Fialová[4]

[1]IT4Innovations National Supercomputing Center, VŠB-Technical University of Ostrava, 17. listopadu 15/2127, 708 33 Ostrava-Poruba, Czech Republic
[2]Department of Applied Mechanics, Faculty of Mechanical Engineering, VŠB-Technical University of Ostrava, 17. listopadu 15/2127, 708 33 Ostrava-Poruba, Czech Republic
[3]Department of Dynamics and Vibration, Institute of Thermomechanics, Czech Academy of Sciences, Dolejškova 1402/5, 182 00 Praha 8, Czech Republic
[4]Victor Kaplan Department of Fluid Engineering, Faculty of Mechanical Engineering, Brno University of Technology, Antonínská 548/1, 601 90 Brno, Czech Republic

Abstract. Technological solution, frequently used to suppress vibrations in rotating machines, consists in adding damping devices between the rotor and its frame. This is enabled by dampers working on the principle of a squeezing thin classical or magnetorheological fluid film. The Navier-Stokes equations, Reynolds equation, and modified Navier-Stokes equations are used to determine the pressure distribution in the thin fluid film. The damping and stiffness coefficients are computed by the developed procedure presented in this paper. The proposed computational approach is based on the perturbation of the synchronous circular whirling motion. The carried-out computational simulations show that the investigated mathematical models of the squeeze film damper and magnetorheological squeeze film damper allowed computation of the damping and stiffness coefficients. It has been found that the stiffness coefficients computed by the proposed mathematical models may be different.

Keywords: Squeeze film damper, Magnetorheological fluid, Hydraulic forces, Navier-Stokes equations, Reynolds equation

1 Introduction

Unbalance of rotating machines is the main source of their lateral vibrations. Technological solution, frequently used to suppress vibrations in rotating machines, consists in adding the damping devices between the rotor and its frame.

The work of the damping devices is based on different, often mutually coupled, physical, mechanical, electric, electromagnetic, piezoelectric, hydraulic, or magneto-rheological principles. A simple device to reduce attenuation of vibration is an elastomeric ring [1] that supports the outer ring of the bearing. The vibration reduction and suppression

* Corresponding author: petr.ferfecki@vsb.cz

Reviewers: *Vladimír* Dekýš, *Zuzana* Murčinková

of the journal bearing instability by the actively controlled journal bearing consists of a movable bushing with the use of piezoactuators as reported in [2]. In paper [3], an electromagnetic damper for the control of the lateral vibration of aero-engines is presented.

On the other hand, squeeze film dampers (SFDs) are based on the mutually coupled hydraulic and mechanical physical principle. SFDs [4] have been used for many years to reduce the amplitude vibration and force transmitted to the foundation in the rotating machinery. The traditional SFDs [4] need to be designed for one free vibration mode shape, which should be eliminated in a rotor layout. Therefore, controllable SFDs working in active [5, 6] or semi active concepts [7-11] have been developed. The concept of semi active working mode is represented by SFDs lubricated by electrorheological [7, 8] or magnetorheological [9-11] fluids.

Due to the physical properties of magnetorheological oils, the magnetorheological SFDs are highly nonlinear damping elements. In order to determine the higher harmonic components in the transient or steady-state response of the rotor system [12-15], it is appropriate to use the frequency spectrums processed by Fourier transform.

The main parts of SFD (Fig. 1a) include two concentric rings with a thin layer of the lubricating film in between. The outer ring is firmly coupled with the damper body while the inner ring is connected with the rotor journal and damper housing by the rolling element bearing and squirrel cage spring, respectively. The spring enables the ring to vibrate in the radial direction but prevents its rotation together with the shaft.

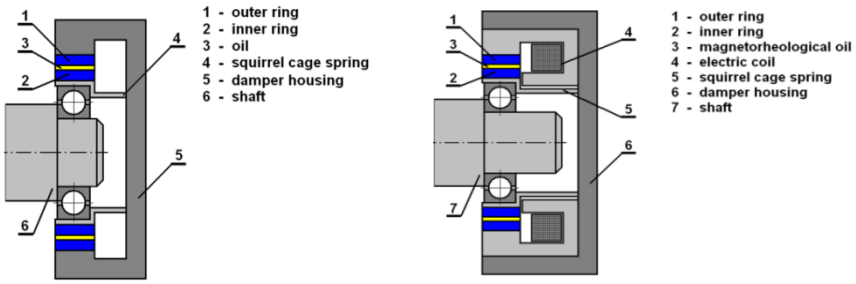

Fig. 1. The scheme of the traditional SFD (a) and magnetorheological SFD (b)

A new concept of the semi-active damping device is represented by SFDs lubricated by magnetorheological oils. The damper body is equipped with an electric coil generating magnetic flux passing through the film of magnetorheological liquid (Fig. 1b). As resistance against its flow depends on magnetic induction, the change of the applied current can be used to control the damping force.

In this paper, the computational procedure for determining the damping and stiffness coefficients of the classical and magnetorheological SFD have been developed and tested with the computational model of the damper presented in [11]. The pressure distribution in SFD is computed with mathematical models of the damper, based on the Navier-Stokes equations (NSE), modified NSE, Reynolds equation (RE), and RE modified for the damper with the short bearing approximation (SBA). A new mathematical model of the magnetorheological SFD with SBA based on the application of a bilinear material has been used to compute the pressure distribution. The carried-out computational simulations show that the developed mathematical models of the traditional SFD and magnetorheological SFD allowed computation of the damping and stiffness coefficients. It has been found that the stiffness coefficients computed by the proposed mathematical models may be different.

2 Pressure distribution in the classical and magnetorheological SFDs

The governing equations for the pressure distribution in the lubricating layer of SFD include NSE and the continuity equation [16], which are set up with the following assumptions: (i) the lubricant behaves as the Newtonian liquid; (ii) the flow in the fluid film is incompressible, laminar, and isothermal

$$\frac{\partial u}{\partial t}+u\frac{\partial u}{\partial x}+v\frac{\partial u}{\partial y}+w\frac{\partial u}{\partial z}=f_{\mathrm{x}}-\frac{1}{\rho}\frac{\partial p}{\partial x}+\frac{\eta}{\rho}\left(\frac{\partial^2 u}{\partial x^2}+\frac{\partial^2 u}{\partial y^2}+\frac{\partial^2 u}{\partial z^2}\right), \tag{1}$$

$$\frac{\partial v}{\partial t}+u\frac{\partial v}{\partial x}+v\frac{\partial v}{\partial y}+w\frac{\partial v}{\partial z}=f_{\mathrm{y}}-\frac{1}{\rho}\frac{\partial p}{\partial y}+\frac{\eta}{\rho}\left(\frac{\partial^2 v}{\partial x^2}+\frac{\partial^2 v}{\partial y^2}+\frac{\partial^2 v}{\partial z^2}\right), \tag{2}$$

$$\frac{\partial w}{\partial t}+u\frac{\partial w}{\partial x}+v\frac{\partial w}{\partial y}+w\frac{\partial w}{\partial z}=f_{\mathrm{z}}-\frac{1}{\rho}\frac{\partial p}{\partial z}+\frac{\eta}{\rho}\left(\frac{\partial^2 w}{\partial x^2}+\frac{\partial^2 w}{\partial y^2}+\frac{\partial^2 w}{\partial z^2}\right). \tag{3}$$

Where x, y, z are the Cartesian coordinates, which define the directions of the fixed frame of reference, u, v, w are the x, y, z components of the velocity, f_{x}, f_{y}, f_{z} are the components of the body force, p is the pressure, t is the time, and ρ and η is the density and dynamic viscosity of the lubricant, respectively.

The equation of continuity represents the conservation of mass, and in the case of the incompressible fluid it can be written in the following form

$$\frac{\partial u}{\partial x}+\frac{\partial v}{\partial y}+\frac{\partial w}{\partial z}=0. \tag{4}$$

RE [16] for the generation of the fluid film pressure can be derived from NSE (1-3) and the continuity equation (4) when taking into account the assumptions of the hydrodynamic lubrication [16, 17]: (i) the lubricant is the Newtonian liquid; (ii) the flow in the fluid film is incompressible, laminar, and isothermal; (iii) the inertial forces in the fluid film are neglected; (iv) the fluid pressure is constant in the radial direction; (v) the inner and outer surface of the damper ring is absolutely rigid and smooth; (vi) the width of the damper gap is small relative to the damper ring radius. Under these assumptions, the pressure distribution in the thin viscous fluid film of SFD is governed by the following RE

$$\frac{\partial}{\partial X}\left(h^3\frac{\partial p}{\partial X}\right)+\frac{\partial}{\partial Z}\left(h^3\frac{\partial p}{\partial Z}\right)=12\eta\frac{\partial h}{\partial t}. \tag{5}$$

Where X, Z denotes the local coordinates describing positions in the lubricating film in the circumferential (X) and axial (Z) direction (Fig. 2).

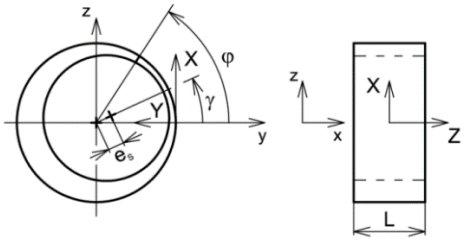

Fig. 2. The damper (xyz) and fluid film (XYZ) coordinate systems

The thickness of the fluid film at a location given by the circumferential coordinate is defined by the relation

$$h=c_0-e_{\mathrm{S}}\cos(\varphi-\gamma), \tag{6}$$

where h denotes the thickness of the fluid film, c_0 is the width of the gap between the inner and outer ring of the damper, e_S is the eccentricity, φ is the circumferential coordinate, and γ is the position angle of the line of the centres (Fig. 2).

It is assumed that the damper is symmetric relative to the plane perpendicular to the journal axis, the damper length to the radii of both rings is small, and the design arrangement of the damper makes it possible to be considered as SBA [17]. For such dampers, the prevailing flow in the lubricating layer occurs in the axial direction and RE (5) reduces to

$$\frac{\partial}{\partial Z}\left(h^3 \frac{\partial p}{\partial Z}\right) = 12\eta \frac{\partial h}{\partial t}. \tag{7}$$

By the double integration of the equation (7), the pressure profile in the axial direction of the damper is obtained in the form

$$p = \frac{6\eta}{h^3}\left(Z^2 - \frac{L^2}{4}\right)\frac{\partial h}{\partial t} + p_A. \tag{8}$$

The boundary condition expressing that the pressure at the ends of the damper is equal to

$$p = p_A, Z = \pm\frac{L}{2}. \tag{9}$$

L is the length of the damper, and p_A is the pressure in the ambient space.

The developed mathematical model of the magnetorheological SFD is based on the assumptions of the hydrodynamic lubrication theory [17] except those for the lubricant. The pressure distribution in the full fluid film is governed by RE adapted for the bilinear material [18]

$$\frac{\partial}{\partial Z}\left(h^3 \frac{\partial p}{\partial Z}\right) = 12\eta_C \frac{\partial h}{\partial t}, \tag{10}$$

$$\frac{\partial}{\partial Z}\left[h^3 \frac{\partial p}{\partial Z} + 3h^2\tau_y + 8\frac{\tau_C^3}{\left(\frac{\partial p}{\partial Z}\right)^2} - 12\frac{\tau_y \tau_C^2}{\left(\frac{\partial p}{\partial Z}\right)^2} - 8\frac{\eta}{\eta_C}\frac{\tau_C^3}{\left(\frac{\partial p}{\partial Z}\right)^2}\right] = 12\eta\frac{\partial h}{\partial t}. \tag{11}$$

Z_C is the axial coordinate, which defines the border between an unsheared region called the core and the region where the shear stress exceeds the τ_y yielding shear stress, τ_C is the shear stress at the core border, and η_C and η are the dynamic viscosities of the lubricant in and outside the core area, respectively. RE (10) is referred to the extent of axial coordinates for which it holds $0 \le Z \le Z_C$, and Eq. (11) describes the pressure distribution in the region where it holds $\partial h/\partial t < 0$ and $0 < Z_C < Z$.

The relation for the axial coordinate Z_C, which defines the border between these two regions, is as follows

$$Z_C = -\frac{\tau_C h^2}{6\eta_C \frac{\partial h}{\partial t}}. \tag{12}$$

The solution of RE adapted to the bilinear material (10, 11) is obtained for the boundary conditions expressing that the pressure at the fluid film ends is equal to the pressure in the ambient space (9).

The yielding shear stress of the magnetorheological fluid, needed for solving the pressure gradient in the region outside the core (11) depends on magnetic induction. Based on the measurements, dependence of the yielding shear stress on magnetic induction can be approximated by a power function [19]

$$\tau_{\mathrm{y}} = k_{\mathrm{y}} B^{n_{\mathrm{y}}}. \tag{13}$$

B is the magnetic induction, and k_{y}, n_{y} are the proportional and exponential material constants of the magnetorheological fluid, respectively.

In the most simple design case, the inner and outer rings of the damper can be considered as a divided core of an electromagnet. Then magnetic induction in the fluid film can be expressed

$$B = k_{\mathrm{B}} \mu_0 \mu_{\mathrm{r}} \frac{I}{h}, \tag{14}$$

where I is the electric current, μ_0 is the vacuum permeability, μ_{r} is the relative permeability of the magnetorheological fluid, and k_{B} is the product of the number of the coil turns and the damping element magnetic efficiency introduced as a ratio of magnetic flux passing through the lubricating layer with respect to the total flux generated by the electric coil. The magnetic efficiency can be determined by computational simulations using a magnetostatic problem utilizing a finite element method [20].

3 Determination of the damping force components

The components of the damping force are obtained by integration of the pressure distribution around the circumference and along the length of the damper

$$f_{\mathrm{y}} = 2R \int_0^{\frac{L}{2}} \int_{\varphi_1}^{\varphi_2} p_{\mathrm{d}} \cos(\varphi) \mathrm{d}\varphi \mathrm{d}Z, \quad f_{\mathrm{z}} = 2R \int_0^{\frac{L}{2}} \int_{\varphi_1}^{\varphi_2} p_{\mathrm{d}} \sin(\varphi) \mathrm{d}\varphi \mathrm{d}Z. \tag{15}$$

$f_{\mathrm{y}}, f_{\mathrm{z}}$ are the y and z components of the damping force, R is the inner ring radius, p_{d} is the pressure distribution, and φ_1, φ_2 are the circumferential integration limits. The pressure distribution and circumferential integration limits are set according to the cavitation model.

The damping forces for SFD with SBA and for both the non-cavitated and cavitated operational regimes can be expressed in the analytical form, the force components expressions of which are given in [4].

The mutual interaction between the magnetorheological damper rings is accomplished by the hydraulic (damping) and magnetic forces. The hydraulic force is produced due to squeezing the magnetorheological fluid film and pushes the rings from each other. On the contrary, the magnetic force attracts. It is induced by the magnetic flux generated in the electric coils. In the paper [21] it was shown that the magnetic attractive force in the magnetorheological damper is much smaller than the hydraulic damping force, and therefore it is neglected in this study.

4 Computational procedure for determining the damping and stiffness coefficients of dampers

The influence of dampers on the performance of the rotating system dynamics has been studied with the mathematical modelling and experimental identification techniques [22].

The damping and stiffness coefficients of SFD and the magnetorheological SFD are obtained under the assumption of a circular centred orbit. The displacement and velocity components for synchronous circular whirling of the inner damper ring are defined by the relations

$$y_{\mathrm{I}} = e \cos(\omega t), \; z_{\mathrm{I}} = e \sin(\omega t), \; v_{\mathrm{I}} = -e\omega \sin(\omega t), \; w_{\mathrm{I}} = e\omega \cos(\omega t), \tag{16}$$

where y_I, z_I are the y and z components of the displacement of the inner damper ring, v_I, w_I are the y and z components of the velocity of the inner damper ring, ω is the whirl frequency, and e is the radius of the orbit.

The perturbed motion is composed by synchronous circular whirling and the superimposed harmonic motion with small amplitude as well as frequency which is higher than the whirl frequency. The components of the perturbed displacements of the inner damper ring are given by the relations

$$y_{I,p} = \left[e + e_p \cos(\omega_p t)\right]\cos(\omega t)\,,\ z_{I,p} = \left[e + e_p \sin\left(\omega_p t\right)\right]\sin(\omega t), \tag{17}$$

where y_{Ip}, z_{Ip} are the perturbed displacements of the inner damper ring in the y and z direction, ω_p is the perturbed whirl frequency, and e_p is the amplitude of the perturbed motion.

The damping and stiffness coefficients may be obtained on the basis of the computed or measured increments of the damping force

$$\Delta\mathbf{f} = \mathbf{f}_p - \mathbf{f},\ \ \Delta\mathbf{f} = \begin{bmatrix}\Delta f_y \\ \Delta f_z\end{bmatrix}, \tag{18}$$

where $\mathbf{f}_p$, $\mathbf{f}$ is the vector of the perturbed and unperturbed damping forces in the stationary reference frame, $\Delta\mathbf{f}$ is the increment of the damping force, and Δf_y, Δf_z are the y and z components of the damping force increment.

Taking into account that the increment of the damping force $\Delta\mathbf{f}$ in the stationary reference frame acting on the inner damper ring can be expressed by the increment of displacement $\Delta\mathbf{q}$ and corresponding increment of the velocity $\Delta\dot{\mathbf{q}}$ of the inner damper ring

$$\Delta\mathbf{f} = \mathbf{B}\,\Delta\dot{\mathbf{q}} + \mathbf{K}\,\Delta\mathbf{q}, \tag{19}$$

$$\mathbf{B} = \begin{bmatrix}b_{y,y} & b_{y,z} \\ b_{z,y} & b_{z,z}\end{bmatrix}, \qquad \mathbf{K} = \begin{bmatrix}k_{y,y} & k_{y,z} \\ k_{z,y} & k_{z,z}\end{bmatrix}, \qquad \Delta\dot{\mathbf{q}} = \begin{bmatrix}\Delta\dot{q}_y \\ \Delta\dot{q}_z\end{bmatrix}, \qquad \Delta\mathbf{q} = \begin{bmatrix}\Delta q_y \\ \Delta q_z\end{bmatrix}.$$

Δq_y, Δq_z, $\Delta\dot{q}_y$, $\Delta\dot{q}_z$ are the y and z components of the increment of displacement and the increment of velocity respectively, $\mathbf{B}$, $\mathbf{K}$ are the matrixes of the damping and stiffness coefficients in the stationary reference frame. In the damping $b_{i,j}$ and stiffness $k_{i,j}$ matrix, all diagonal terms are called direct coefficients and off-diagonal terms are called cross-coupled terms.

The increment of displacement $\Delta\mathbf{q}$ and corresponding increment of the velocity $\Delta\dot{\mathbf{q}}$ of the right-hand side of the equation (19) is obtained by computations for predefined kinematic parameters of the unperturbed and perturbed motion. Therefore, the unknown damping and stiffness coefficients are solved from linear equations in the following form

$$\begin{bmatrix}b_{y,y} \\ b_{y,z} \\ k_{y,y} \\ k_{y,z}\end{bmatrix} = \mathbf{A}^+ \begin{bmatrix}\Delta f_{y,1} \\ \vdots \\ \Delta f_{y,n}\end{bmatrix},\ \begin{bmatrix}b_{z,y} \\ b_{z,z} \\ k_{z,y} \\ k_{z,z}\end{bmatrix} = \mathbf{A}^+ \begin{bmatrix}\Delta f_{z,1} \\ \vdots \\ \Delta f_{z,n}\end{bmatrix},\ \ \mathbf{A} = \begin{bmatrix}\Delta\dot{q}_{y,1} & \Delta\dot{q}_{z,1} & \Delta q_{y,1} & \Delta q_{z,1} \\ \vdots & \vdots & \vdots & \vdots \\ \Delta\dot{q}_{y,n} & \Delta\dot{q}_{z,n} & \Delta q_{y,n} & \Delta q_{z,n}\end{bmatrix}. \tag{20}$$

The damping and stiffness coefficients in the stationary reference frame are a periodical function of time and due to the increase in both accuracy of their computation and the numerical stability of the matrix $\mathbf{A}$, the coefficients must be set during one period at a number of the time points ($n > 20$). The Moore-Penrose pseudoinverse ($\mathbf{A}^+$) is applied for solving the linear equations (20).

5 Computational simulations

Applicability of the developed methodology is demonstrated on the magnetorheological SFD, presented in [11]. Its photography is drawn in Fig. 3.

Fig. 3. The image of the investigated magnetorheological SFD

The technological parameters of the investigated magnetorheological SFD are as follows: the radius of the outer ring is 76 mm, length of the damper is 44 mm, width of the gap between the inner and outer ring of the damper is 1 mm, oil dynamic viscosity not affected by a magnetic field is 0.1 Pa·s, oil dynamic viscosity in the core is 500 Pa·s, magnetorheological oil density is 970 kg·m^{-3}, oil relative permeability is 5, damper design parameter is 60, and magnetorheological oil proportional and exponential material constants are 15 000 Pa·T^{-2} and 2, respectively.

The parameters of synchronous circular whirling of the inner damper ring are defined as follows: the whirl frequency is 1800 rpm, radius of orbit is 0.05 mm, perturbed whirl frequency is 18 000 rpm, and amplitude of the perturbed motion is 0.05 μm.

The task was to study the damping and stiffness coefficients (i) for the traditional SFD (the magnetorheological damper coils are not connected to current supply) and (ii) for the magnetorheological SFD.

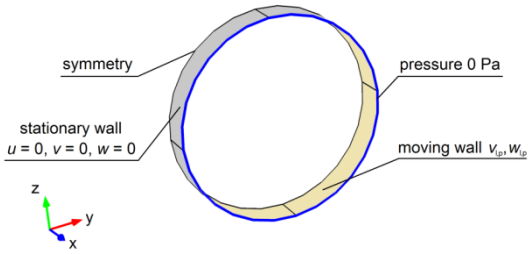

Fig. 4. Schematic representation of the SFD geometry with applied boundary conditions; v_{lp}, w_{lp} are the y and z components of the perturbed velocity

In this work, the commercial COMSOL software was used for solving the forces acting in SFD. The orbit radius is equal to 5% of the width of the gap between the inner and outer ring of the damper. Due to the small radius of circular whirling, the changes in the domain boundaries are negligible, the shape of the fluid domain is almost the same and therefore only one geometry model in COMSOL is used. The three-dimensional geometry of the damper filled with oil is simplified to the thin cylinder film (Fig. 4). The boundary conditions were defined in the form of ambient pressure at the outlet, symmetry at the half of the damper length, stationary outer ring, and movable inner damper ring (Fig. 4). The fluid is assumed to be incompressible, gravity forces are not taken into account, and the Reynolds number is equal to 1.8, and therefore the viscous model is set to laminar. NSE (1-3) and the continuity equation (4) are numerically solved using a time-varying solver.

The pressure distribution on the surface of the lubricating film for the non-cavitated (a) and cavitated (b) operational regime of the traditional SFD is depicted in Fig. 5. The location of the inner ring is offset in the horizontal (y) direction by 0.05 mm. The pressure distribution is almost constant in the radial direction, which clearly shows that the basic assumption of RE is satisfied.

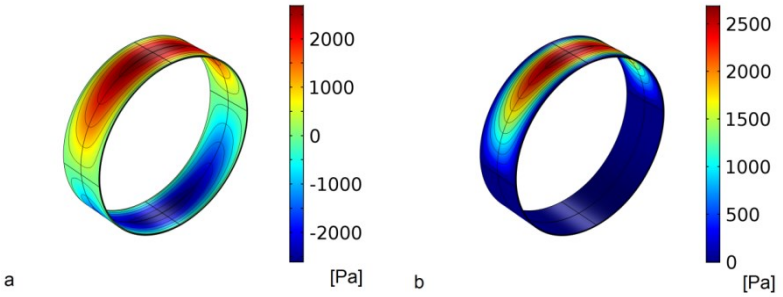

Fig. 5. Pressure distribution in the non-cavitated (a) and cavitated (b) operational regime of SFD

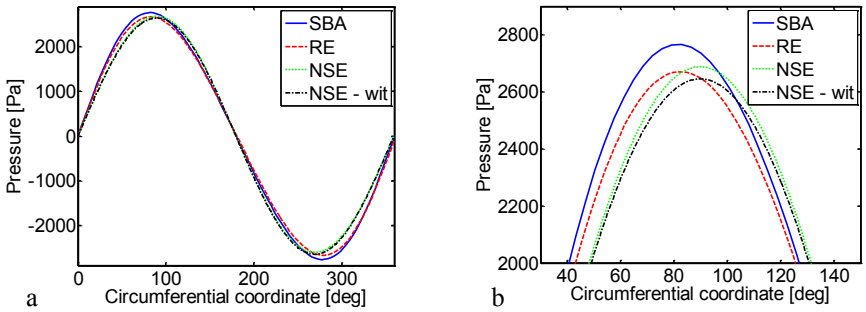

Fig. 6. Pressure distribution in the damper middle plane (a) and the detail of the maximum pressure distribution (b); NSE-wit (Navier-Stokes equations - without inertial terms)

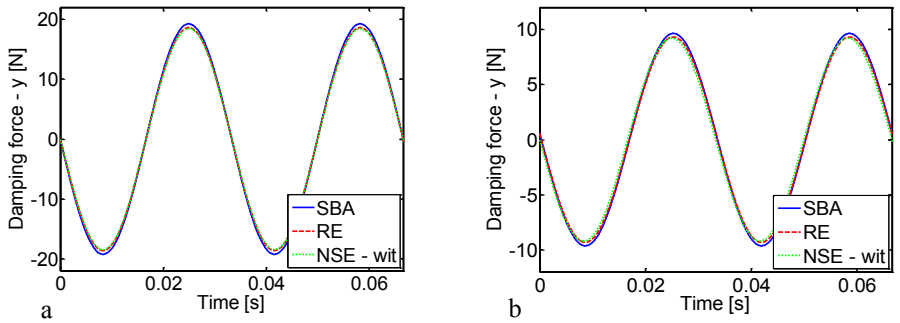

Fig. 7. Time history of the damping force in the horizontal direction in the non-cavitated (a) and cavitated (b) operational regime of SFD

The pressure distribution in the damper middle plane for the non-cavitated operational regime computed by means of several mathematical models of SFD is drawn in Fig. 6. The small differences in the amplitude and phase shift of the pressure distribution are determined between both mathematical models based on NSE. These differences are caused by negligence of the inertial effects in the NSE-wit mathematical model of the damper. The pressure distribution computed using the mathematical models (SBA, RE, and NSE-wit) of the damper neglecting the inertial forces is almost identical.

The time history of the damping force in the horizontal direction is depicted in Fig. 7. It is evident that the damping force for the non-cavitated operational regime is higher than the force related to the cavitated operational regime of SFD. The mathematical model of the damper with the assumptions of SBA arrives at the small increase in the damping force. And in this case, the flow in the damper is only in the axial direction. On the contrary, the mathematical model with NSE-wit arrives at a small reduction of the amplitude of the damping force and flow in the damper is three-dimensional.

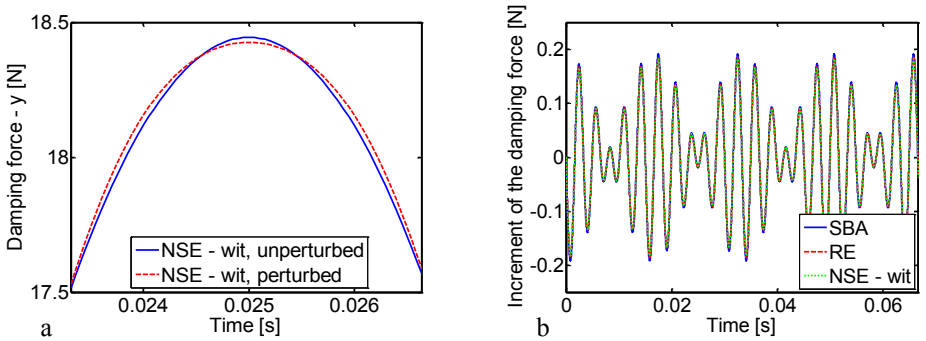

Fig. 8. Detail of the time history of the damping force (a) and time history of the increment of the damping force in the horizontal direction (b)

In order to compute the damping and stiffness coefficients, the perturbed motion is considered and the unperturbed and perturbed damping force is plotted in Fig. 8a. The corresponding increment of the damping force is depicted in Fig. 8b. SFD is operating in the non-cavitated regime. Fig. 8b shows that the increment of the damping force for the three mathematical models (SBA, RE, NSE-wit) of the damper is almost the same.

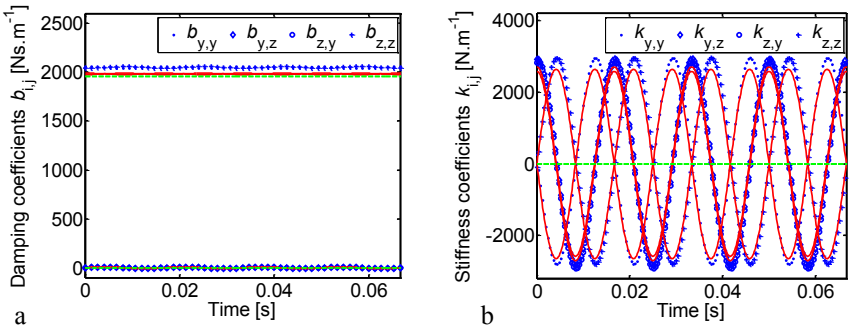

Fig. 9. Time history of the damping (a) and stiffness (b) coefficients in the non-cavitated regime of SFD; SBA (blue symbols), RE (continuous red line), NSE-wit (dashed green line)

The time-varying damping and stiffness coefficients in the stationary reference frame of SFD and the three mathematical models (SBA, RE, NSE-wit) of the damper are depicted in Figs. 9 and 10 (the non-cavitated regime and cavitated operational regime, respectively). The magnitude of the direct damping coefficients for the non-cavitated regime is greater than the one for the cavitated operational regime. The direct damping coefficients are almost equal for the three mathematical models (SBA, RE, NSE-wit). The cross-coupled coefficients of the damping are the same size and its value of magnitude is small for the mathematical models based on SBA and RE. For the NSE-wit model, the cross-coupled coefficients are equal to zero. The results show that all stiffness coefficients are equal to zero only for NSE-wit mathematical model of the damper. This applies to the both SFD

operating regimes. For the non-cavitated and cavitated operational regimes of SFD (Fig. 9, Fig. 10), the values of the direct stiffness coefficients are different in comparison with the damping coefficients.

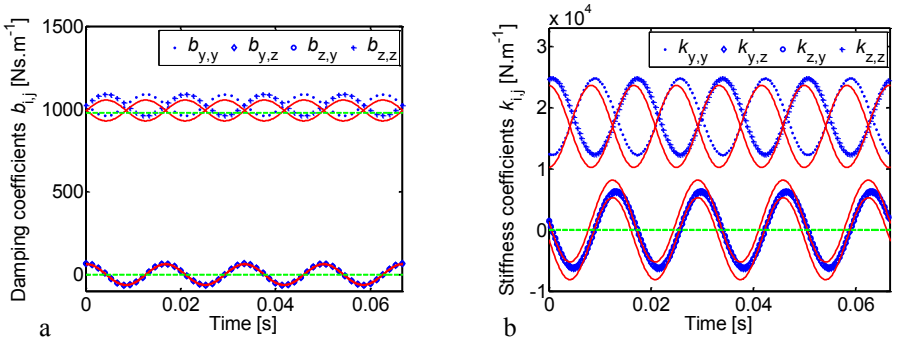

Fig. 10. Time history of the damping (a) and stiffness (b) coefficients in the cavitated operational regime of SFD; SBA (blue symbols), RE (continuous red line), NSE-wit (dashed green line)

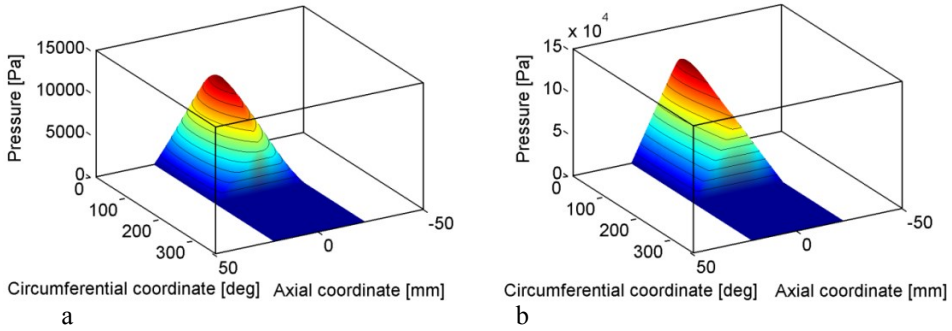

Fig. 11. Pressure distribution in the cavitated operational regime of the magnetorheological SFD, $I = 0.25$ A (a), $I = 1.0$ A (b)

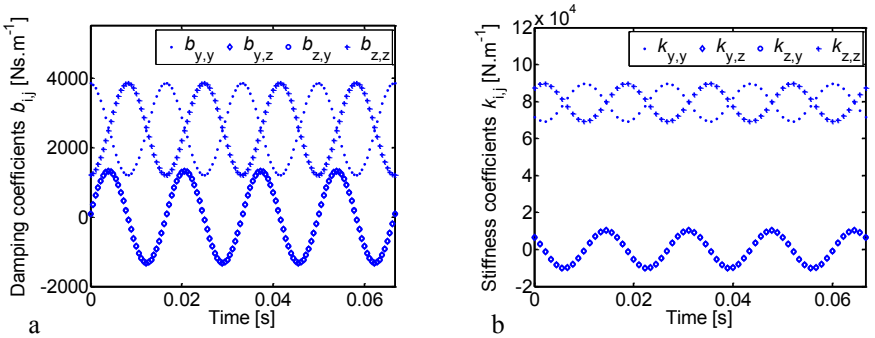

Fig. 12. Time history of the damping (a) and stiffness (b) coefficients in the stationary reference frame of the magnetorheological SFD, $I = 0.25$ A

The mathematical model of the magnetorheological SFD with the assumptions of the SBA and based on the application of a bilinear material (10, 11) has been used. The location of the inner ring is offset in the horizontal (y) direction by 0.05 mm. The pressure distribution in the area of the oil film for two magnitudes of the applied current is drawn in Fig. 11. The results show that a rising electric current increases the magnitude of the pressure.

The corresponding time-varying damping and stiffness coefficients in the stationary reference frame of the magnetorheological SFD are depicted in Fig. 12 and Fig. 13. The magnetorheological damper is operating in the cavitated regime. The higher the value of the current supplied in the coils the larger the magnitude of the damping and stiffness coefficients.

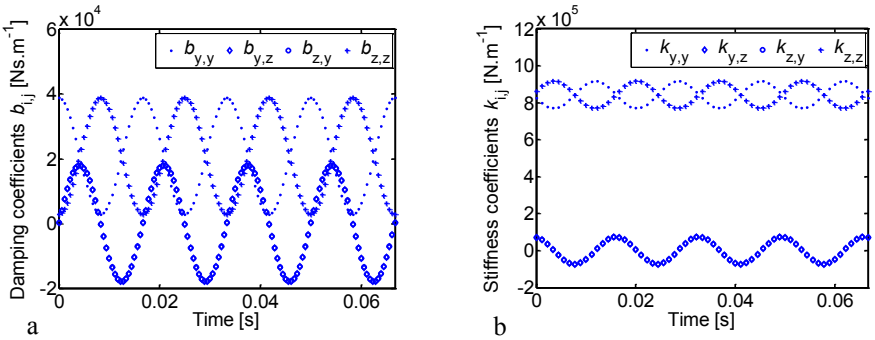

Fig. 13. Time history of the damping (a) and stiffness (b) coefficients in the stationary reference frame of the magnetorheological SFD, I = 1.0 A

Conclusion

The development of a novel computational procedure for computing the damping and stiffness coefficients of the traditional SFD and magnetorheological SFD, learning more about the effect of the inertial forces in SFD on the pressure distribution and damping forces, and the knowledge about the behaviour of the damping and stiffness coefficients are the principal contributions of this article.

Mathematical models of the damper based on NSE, modified NSE, RE, and RE modified for the damper with SBA were implemented for computation of the pressure distribution and the damping forces. It was found that the stiffness coefficients computed by the proposed mathematical models in SFD may be different.

The mathematical model of the magnetorheological SFD with SBA, where the magnetorheological fluid is represented by the bilinear material, has been used to achieve a more accurate description and increased computational stability. The simulation results show that with the rising electric current the magnitude of the damping and stiffness coefficients of the magnetorheological SFD increases.

This work has been supported by The Ministry of Education, Youth and Sports from the National Programme of Sustainability (NPU II) project „IT4Innovations excellence in science - LQ1602“, by the Czech Science Foundation 15-06621S, and by the Specific Research SP2017/136.

References

1. C. C. Thomazi, M. B. dos Santos, F. P. L. Neto, *Numerical analysis of a rotor-bearing system supported by elastomeric dampers.* Rev. Cient. **3**, 79-95 (2016)
2. J. Tůma, J. Šimek, J. Škuta, J. Los, *Active vibrations control of journal bearings with the use of piezoactuators*. Mech. Syst. Signal Process. **36**, 618-629 (2013)
3. A. Tonoli, N. Amati, A. Bonfitto, M. Silvagni, B. Staples, E. Karpenko, *Design of electromagnetic dampers for aero-engine applications*. J. Eng. Gas Turbines Power **132**, 112501 (2010)
4. J. M. Vance, *Rotordynamics of turbomachinery*. John Willey & Sons (1988)

5. A. El-Shafei, *Active control algorithms for the control of rotor vibrations using hybrid squeeze film dampers*. J. Eng. Gas Turbines Power **124**, 598-607 (2002)
6. H. R. Heidari, P. Safarpour, *Design and modeling of a novel active squeeze film damper*. Mech. Mach. Theory **105**, 235-243 (2016)
7. A. Bouzidane, M. Thomas, *An electrorheological hydrostatic journal bearing for controlling rotor vibration*. Comput. Struct. **86**, 463-472 (2008)
8. Y. Sun, M. Thomas, *Control of torsional rotor vibrations using an electrorheological fluid dynamic absorber.* J. Vib. Control **17**, 1253-1264 (2011)
9. C. Carmignani, P. Forte, E. Rustighi, *Design of a novel magneto-rheological squeeze-film damper*. Smart Mater. Struct. **15**, 164-170 (2006)
10. G. J. Wang, N. Feng, G. Meng, E. J. Hahn, *Vibration control of a rotor by squeeze film damper with magnetorheological fluid*. J. Intell. Mater. Syst. **17**, 353-357 (2006)
11. J. Zapoměl, P. Ferfecki, P. Forte, *A computational investigation of the transient response of an unbalanced rigid rotor flexibly supported and damped by short magnetorheological squeeze film dampers*. Smart. Mater. Struct. **21**, 105011 (2012)
12. A. Sapietová, V. Dekýš, *Dynamic analysis of rotating machines in MSC.ADAMS.* Procedia Eng. **136**, 143-149 (2016)
13. V. Dekýš, P. Novák, O. Dvouletý, L. Radziszewski, *The contribution to the analysis of the run up test.* Procedia Eng. **136**, 181-186 (2016)
14. V. Dekýš, A. Sapietová, O. Števka, *Understanding of the dynamical properties of machines based on the interpretation of spectral measurements and FRF*. Appl. Mech. Mater. **486**, 106-112 (2014)
15. V. Dekýš, P. Kalman, P. Hanák, P. Novák, Z. Stankovičová, *Determination of vibration sources by using STFT*. Procedia Eng. **177**, 496-501 (2017)
16. A. Z. Szeri, *Tribology: Friction, lubrication, and wear.* Hemisphere Publishing Corporation (1980)
17. Y. Hori, *Hydrodynamic lubrication*. Springer-Verlag (2006)
18. J. Zapoměl, P. Ferfecki, J. Kozánek, *Modelling of magnetorheological squeeze film dampers for vibration suppression of rigid rotors.* Int. J. Mech. Sci. **127**, 191-197 (2017)
19. O. Marinică, D. Susan-Resiga, F. Bălănean, D. Vizman, V. Socoliuc, L. Vékás, *Nano-micro composite magnetic fluids: Magnetic and magnetorheological evaluation for rotating seal and vibration damper applications*. J. Magn. Magn. Mater. **406**, 134-143 (2016)
20. P. Ferfecki, J. Zapoměl, J. Kozánek, *Analysis of the vibration attenuation of rotors supported by magnetorheological squeeze film dampers as a multiphysical finite element problem*. Adv. Eng. Softw. **104**, 1-11 (2017)
21. P. Ferfecki, J. Zapoměl, M. Marek, *Multi-physical analysis of the forces in the flexible rotor supported by the magnetorheological squeeze film dampers*. Adv. Mech. Design II. Mech. Mach. Sci. **44**, 89-95 (2017)
22. R. Tiwari, A. W. Lees, M. I. Friswell, *Identification of dynamic bearing parameters: A review*. Shock Vib. Dig. **36**, 99-124 (2004)